

Determining vortex chirality in ferromagnetic ring by lateral nonlocal spin valve

D. C. Chen, Y. D. Yao, J. K. Wu, C. Yu, and S. F. Lee

Citation: [Journal of Applied Physics](#) **103**, 07F312 (2008); doi: 10.1063/1.2832866

View online: <http://dx.doi.org/10.1063/1.2832866>

View Table of Contents: <http://scitation.aip.org/content/aip/journal/jap/103/7?ver=pdfcov>

Published by the [AIP Publishing](#)

Articles you may be interested in

[Chirality control of magnetic vortex in a square Py dot using current-induced Oersted field](#)

Appl. Phys. Lett. **99**, 242507 (2011); 10.1063/1.3669410

[Surface enhanced spin-flip scattering in lateral spin valves](#)

Appl. Phys. Lett. **96**, 022513 (2010); 10.1063/1.3291047

[Spin-current-induced dynamics in ferromagnetic nanopillars of lateral spin-valve structures](#)

J. Appl. Phys. **105**, 07D110 (2009); 10.1063/1.3058621

[Magnetization process of a single magnetic ring detected by nonlocal spin valve measurement](#)

J. Appl. Phys. **101**, 126102 (2007); 10.1063/1.2745311

[Determination of magnetic vortex chirality using lateral spin-valve geometry](#)

Appl. Phys. Lett. **87**, 172506 (2005); 10.1063/1.2120911



Re-register for Table of Content Alerts

Create a profile.



Sign up today!



Determining vortex chirality in ferromagnetic ring by lateral nonlocal spin valve

D. C. Chen,^{1,a)} Y. D. Yao,² J. K. Wu,² C. Yu,³ and S. F. Lee³

¹Department of Materials Science and Engineering, National Chiao Tung University, Hsinchu, Taiwan 300

²The Department of Materials Engineering, Tatung University, Taipei, Taiwan 104

³Institute of Physics, Academia Sinica, Taipei, Taiwan 11529

(Presented on 6 November 2007; received 22 September 2007; accepted 24 October 2007; published online 8 February 2008)

We demonstrate detecting chirality of vortex state in a magnetic ring by lateral nonlocal spin-valve (NLSV) measurement. A Permalloy (Py) ring, a Py narrow wire, and copper contacts were used as spin injector, detector, and the normal-metal diffusive channel, respectively. By comparing the anisotropic magnetoresistance loop of the individual ring with NLSV loop, the vortex chirality and the related switching field of the ring can be determined. Both onion-to-vortex transition field and vortex chirality were found to alternate in both the same and different current probe arrangements on the magnetic ring. © 2008 American Institute of Physics. [DOI: 10.1063/1.2832866]

Ferromagnetic ring structure has raised a great motivation to study due to its potential application¹ on spintronics and the physical phenomenon of the magnetization reversal process, which has been clearly studied.^{2–5} The magnetization reversal process of a ferromagnetic ring goes through head-to-head onion state via the vortex state (or flux closure state) and then to the reverse onion state. The whole detailed process and its physical origin has been well described and explained.⁶ Due to the advantage of the absence of stray field fluxed outside the ferromagnetic material, the chirality of the vortex state could be used as a promising memory element to identify the “1” or “0” digital signal defined by the spin signal of counterclockwise (CCW) or clockwise (CW) direction of the vortex state. Therefore, the chirality determination of the vortex state plays an important role in serving as a memory element in magnetoelectronic devices. To efficiently detect the vortex state in a ring structure, we used lateral nonlocal spin valve (NLSV), in which the phenomena of electron spin injection, diffusion, accumulation, and detection have been well investigated.^{7–10} Compared with conventional measurement, the nonlocal measurement diminishes most signals from anisotropic magnetoresistance (AMR), spin-dependent scattering, and Hall effect. Instead, it extracts pure information of spin accumulation from the diffusive normal-metal channel. With this advantage, Kimura and Otani¹¹ first demonstrated the determination of magnetic vortex chirality in a ferromagnetic ring by using lateral spin valve. The investigation successfully demonstrated determining the magnetic vortex chiralities by using nonlocal measurement without charge current in the magnetic ring. In the present investigation, however, electric current was introduced into magnetic ring and some effects due to different current probe arrangement were observed.

In this work, a lateral NLSV structure was constructed (Fig. 1). A Py ring, a Py narrow wire, and Copper contacts were used as spin injector, detector, and the normal-metal diffusive channel, respectively. Electron-beam lithography

and lift-off technique were used to fabricate the structure. The ring (2 μm in outer diameter, 0.3 μm in width, and 30 nm in thickness) and the narrow wire (0.1 μm in width and 30 nm in thickness) were first deposited on SiO_2/Si substrate by using dc magnetron sputtering in which the base pressure and the working pressure were 5×10^{-7} and 1.1×10^{-3} Torr, respectively. The spacing between the ring and the wire was 350 nm. Before depositing copper contacts, the Py surface was well cleaned by means of ion milling at a discharge bias of 3 kV for 3.5 min and at the working pressure of 1×10^{-5} Torr. Then, without breaking the vacuum, the Cu probes (60 nm in thickness) were fabricated to connect the ring and the wire to the pad leads by means of the same fabrication process used for the patterned Py ring and wire films. The MR measurement was performed at 44 K. An ac resistance bridge instrument (with built-in lock-in technique) was used to provide a current with the frequency of 16 Hz and the magnitude of 0.5 mA. A sweeping magnetic field was applied parallel to longitudinal direction of the Py wire to alter the magnetizations of the ring and the wire during MR measuring with a sampling step of 3 Oe.

To compare with NLSV signals, the AMR of the individual Py ring was also measured by employing Cu contacts

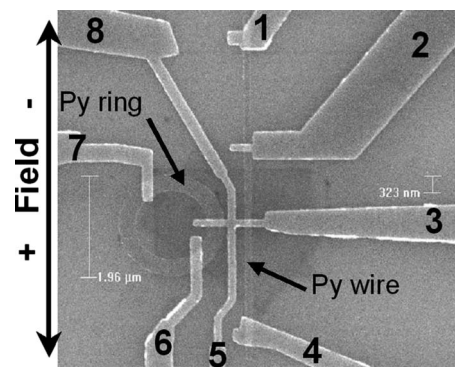


FIG. 1. Scanning electron microscopy (SEM) image of the lateral spin-valve structure. The Permalloy (Py) ring and the Py narrow wire are indicated by the arrows. Cu contacts are labeled as 1–8. The double-headed arrow on the left side defines the direction of applied field.

^{a)}Electronic mail: dcchen@phys.sinica.edu.tw.

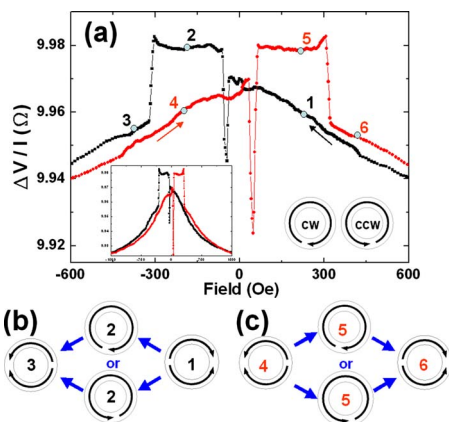


FIG. 2. (Color online) (a) The AMR loop of the ring. The arrows indicate the direction of the proceeding process on the loop. The left inset shows the full range of field -1500 – $+1500$ Oe. Vortex directions are schematically indicated in the right inset. Each number with its solid circle is employed to represent each magnetization state and the sequence in process, which is also shown in schematic diagram [(b) and (c)], in which, the magnetization reversal process is schematically represented.

7 and 5 as voltage probes and contacts 6 and 8 as current probes. Here, the arrangement of current probes and the amplitude of the current were respectively set identical to that in NLSV measurement. Therefore, the reversal processes of the Py ring at the two different measurements (NLSV and AMR) would not be obviously various due to possible current induced effect. The AMR loop for the ring is shown in Fig. 2(a). Since the current flows along the perimeter of the ring, the MR would be at the highest resistance while all magnetic moments are aligned to the perimeter direction (current parallel to moment), and at lower resistance while some or even most of the moments are out of the perimeter direction. Furthermore, the magnetic moments' vector components with higher magnitude are aligned to the direction of stronger applied field (near saturation). At the weaker field, however, components with higher magnitude are aligned to the perimeter direction of the ring (onion state or vortex state) since the field no longer strong enough to overcome the shape anisotropic field of the ring. Hence, the AMR behavior of the ring reveals that the resistance is relatively low at stronger field and high at weaker one. However, the detailed reversal process behaves more complicatedly during the switching of magnetization states. At the field -50 to -80 Oe, a dramatically decrease and the subsequent increase in resistance appear respectively due to the expansion and annihilation of the two walls in onion state [state 1 in Figs. 2(a) and 2(b)]. After completing the annihilation of the two walls, the magnetization reversal process goes into vortex state (state 2) in which all of the moments are parallel along the perimeter direction of the ring, and the resistance increases to higher than that at onion state. With the field exceeding at -300 Oe, the vortex state changes into reverse onion state (state 3). Hence, the MR shows an abrupt drop at -300 Oe and maintains decreasing with field increasing toward negative direction. At vortex state, however, CW and CCW vortices occupy the common resistance level. Therefore, the AMR loop of the individual ring provides no crucial information to distinguish the chiralities of the vortex state. The AMR loop of the ring in

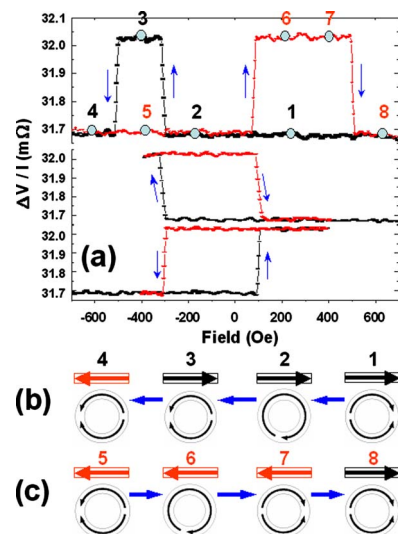


FIG. 3. (Color online) (a) The full MR loop of the NLSV device (top curve) and the minor loops (middle and bottom curves). The arrows indicate the direction of the proceeding process on the loops. The numbers [correspondent with that in (b) and (c)] represent the sequence in reversal process and the magnetic configurations of the NLSV. (b) Magnetic configurations in the reversal process from positive field to negative. (c) The same as (b) but in reverse sweep.

the present study reveals a tendency in accordance with that in the investigation.¹²

To perform NLSV measurement, current probes were set as 6 and 8, and voltage probes as 5 and 2. One of the NLSV MR full loops (field exceeding the switching field of the Py wire) is shown in Fig. 3(a) (top curve). It reveals a clear spin-valve signal without other AMR effect. Starting with the sweeping from the positive field to negative one (forward sweep), the resistance is at low level during the process from the onion state [spin-valve configuration 1 in Figs. 3(a) and 3(b)] to -300 Oe. Here, the field -300 Oe is in accordance with that in the previous AMR loop of the individual ring. This indicates the magnetizations of the narrow wire and the region near the Cu/ring interface is maintained at parallel configuration until the switching for vortex state to reverse onion state. Hence, the vortex state (configuration 2) would be CW direction. After the vortex state switches at -300 Oe into the reverse onion state, the configuration of the spin-valve magnetizations switches to antiparallel state and results in an increase in resistance with a clear step at -300 Oe. The high resistance level remains until -510 Oe (configuration 3). After -510 Oe, the magnetization of the narrow wire switches to the opposite direction, and spin-valve configuration switches to parallel state (configuration 4). The resistance consequently changes back to the originally low level, hence, a plateau from -300 to -510 Oe forms in the NLSV loop. At the reverse sweep (from negative to positive field), however, the NLSV signal shows asymmetric with the former. Since the plateau (high resistance level) is from 80 Oe (correspondent with that in the ring AMR) to 510 Oe, the spin-valve configuration would be antiparallel during the vortex state. Consequently, the vortex state must be in CW [configuration 6 in Figs. 3(a) and 3(c)] so that the magnetization near the Cu/ring interface would be antiparallel to the narrow wire. Furthermore, the reverse onion state still keeps

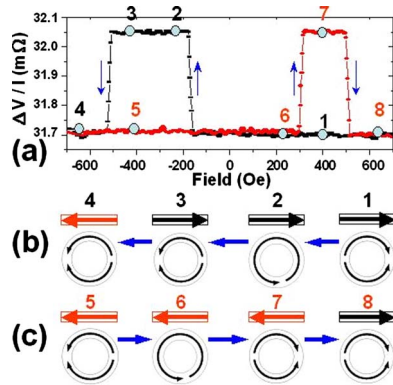


FIG. 4. (Color online) Another NLSV loop for the same probe arrangement as in Fig. 3. The depiction for the numbers and arrows are the same as in Fig. 3.

the spin-valve configuration antiparallel (configuration 7). Hence, the resistance remains high level until the switching of the Py wire at 510 Oe. The measurement of minor loop was also performed to confirm the MR behavior of NLSV, as shown in Fig. 3(a) (middle and bottom curves). The result shows the same switching fields and the same vortex chiralities with that of the full loop (up curve).

The other kind of NLSV loops for the present probe arrangement shows different behaviors of reversal process (Fig. 4). The two plateaus form at the regions from -150 to -510 Oe and 300 – 510 Oe in the forward sweep and reverse sweep, respectively. This infers that the vortex states are both CCW for both sweep processes. Furthermore, the switching field for onion state to vortex state changes to -150 Oe in the forward sweep. For the present probe arrangement, full loop was repeated for five times, and minor loop (applied field lower than switching field of the Py wire) also five times for each of the two directions at which the magnetization of Py wire were held. The result of the ten minor loops (20 sweeps) indicates that the chiralities are all CW regardless of the sweeping direction (forward or backward sweep) and the direction at which the magnetization of Py wire was held. For the five full loops, three of them are CW-CW loop (CW in forward sweep and CW in backward sweep), as shown in Fig. 3(a) (up curve), and the other two are CCW-CCW loop (CCW in both forward and backward sweeps), as shown in Fig. 4. Another NLSV measurement was also performed with replacing current probe 6 by 7 and maintain the others unchanged.

The number of NLSV loops repeated is identical to that in the previous probe arrangement. Within the five full loops, four loops exhibit CCW-CW loop shown in Fig. 5(a), and the other one behaves CCW-CCW loop in Fig. 5(b). For the four CCW-CW loops, both plateaus are 150 – 510 Oe in absolute value. This means the switching field for onion state to vortex state is 150 Oe, different from that (80 Oe) in the previous probe arrangement. In the CCW-CCW loop, the plateaus are from -150 to -510 and 315 to 510 Oe for forward and backward sweeps, respectively. Hence, the switching field for vortex state to reverse onion state is near 315 Oe higher than that in the previous probe arrangement. As the results from the minor loop measurement, ten loops are all CCW-CW regardless of the sweeping direction and the di-

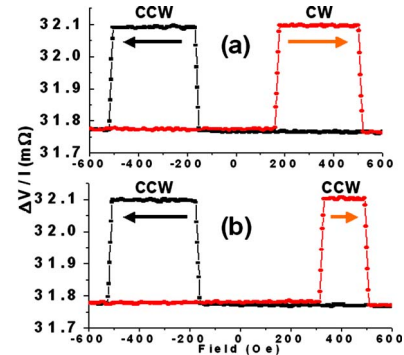


FIG. 5. (Color online) The NLSV loops for the probe arrangement in which the current probes were set as 7 and 8. The depictions for the arrows are the same with that in Figs. 3 and 4. (a) The CCW-CW loop: CCW in sweep from positive to negative field (forward sweep); and CW in the opposite (backward) sweep. (b) The CCW-CCW loop: CCW in both forward and backward sweeps.

rection at which the magnetization of Py wire was held.

Here, we briefly summary the observed results. In the same one probe arrangement, the switching fields of the onion-to-vortex transition are roughly near a certain value with a distribution of small range. The current probes connected to Py ring are not arranged at symmetric positions on the ring and, hence, the current distribution is not uniform over the entire Py ring. Consequently, the heat generated by current could neither be uniform. Therefore, the occurrence of CW and CCW vortex could not occupy the same possibility. Besides, the two different current probe arrangements generate different thermal distribution over the ring. This could account for the dependence of switching field and chirality upon current probe arrangement.

This work demonstrates detecting chirality of vortex state in a magnetic ring by lateral NLSV measurement. Both onion-to-vortex transition field and vortex chirality were found to alternate in both the same and different current probe arrangements. The results could give rise to a potential topic of systematically studying the effect of probe arrangement on vortex chirality.

This work was financially supported by the National Science Council of Taiwan under Grant No. NSC 95-2112-M-036-002-MY3.

- ¹J.-G. Zhu, Y. Zheng, and G. A. Prinz, *J. Appl. Phys.* **87**, 6668 (2000).
- ²J. Rothman, M. Kläui, L. Lopez-Diaz, C. A. F. Vaz, A. Bleloch, J. A. C. Bland, Z. Cui, and R. Speaks, *Phys. Rev. Lett.* **86**, 1098 (2001).
- ³S. P. Li, D. Peyrade, M. Natali, A. Lebib, Y. Chen, U. Ebels, L. D. Buda, and K. Ounadjera, *Phys. Rev. Lett.* **86**, 1102 (2001).
- ⁴M. Kläui, C. A. F. Vaz, J. A. C. Bland, W. Wernsdorfer, G. Faini, and E. Cambril, *Appl. Phys. Lett.* **81**, 108 (2002).
- ⁵T. Uhlir and J. Zweck, *Phys. Rev. Lett.* **93**, 047203 (2004).
- ⁶T. A. Moore, T. J. Hayward, D. H. Y. Tse, J. A. C. Bland, F. J. Castaño, and C. A. Ross, *J. Appl. Phys.* **97**, 063910 (2005).
- ⁷M. Johnson and R. H. Silsbee, *Phys. Rev. Lett.* **55**, 1790 (1985).
- ⁸M. Johnson and R. H. Silsbee, *Phys. Rev. Lett.* **37**, 5326 (1988).
- ⁹F. J. Jedema, A. T. Filip, and B. J. van Wees, *Nature (London)* **410**, 345 (2001).
- ¹⁰F. J. Jedema, M. S. Nijboer, A. T. Filip, and B. J. van Wees, *Phys. Rev. B* **67**, 085319 (2003).
- ¹¹T. Kimura and Y. Otani, *J. Appl. Phys.* **87**, 172506 (2005).
- ¹²M.-F. Lai, Z.-H. Wei, C.-R. Chang, J. C. Wu, J. H. Kuo, and J.-Y. Lai, *Phys. Rev. B* **67**, 104419 (2003).